Review of Capacitive Atmospheric Icing Sensors

Umair Najeeb Mughal[1], Muhammad Shakeel Virk[2], Mohamad Yazid Mustafa[3]
High North Technology Center, Department of Technology
Narvik University College
Narvik, Norway
Email: unm@hin.no[1], msv@hin.no[2], myfm@hin.no[3]

***Abstract*—The application of capacitive sensing technique is widely distributed in different physical domains primarily because of the diversity in dielectric permittivity and due to its minimum loading error and inertial effects. Atmospheric ice is a complex mixture of water, ice and air which is reflected in its complex dielectric constant. There are many existing atmospheric icing sensors but only few are based on their complex dielectric permittivity measurements. This technique is very suitable because the capacitive variation in this mixture is due to the reorientation of water dipole in the electromagnetic radiation's oscillating field. Depending on the frequency, the dipole may move in time to the field, lag behind it or remain apparently unaffected. This variation is clearly reflected on the cole cole diagram which is a measure of the relaxation frequency. This paper is a review of some capacitive sensing technique in general but based upon dielectric variations and some existing capacitive based atmospheric ice sensing techniques. It is emphasized that the capacitive method proposed by Jarvenin provides maximum atmospheric icing parameters hence future atmospheric icing sensors may utilize the proposed technique with some modifications to further reduce the loading errors.**

Keywords-Atmospheric ice; Sensor; Polar molecule; Dielectric.

I. INTRODUCTION

A. Atmospheric icing

Atmospheric icing is the term used to describe the accretion of ice on structures or objects under certain conditions. This accretion can take place either due to freezing precipitation or freezing fog. It depends mainly on the shape of the object, wind speed, temperature, liquid water content (amount of liquid water in a given volume of air) and droplet size distribution (conventionally known as the median volume diameter).

The major *effects of atmospheric icing* on structure are the static ice loads, wind action on iced structure and dynamic effects.

Generally an icing event is defined as period of the time when the temperature is below $0°C$ and the relative humidity is above 95%. Ice accretion can be defined as, *any process of ice build up and snow accretion on the surface of objects exposed to the atmosphere'* [6]. Atmospheric icing is traditionally classified according to two different processes [6] and are shown in Fig. 1(a).

Table I: TYPICAL PROPERTIES OF ACCRETED ATMOSPHERIC ICE [5]

Type of ice	Density (kg/m^3)	General appearance	
		Colour	*Shape*
Glaze	900	transparent	evenly distributed/icicles
Wet snow	300-600	white	evenly distributed/eccentric
Hard rime	600-900	opaque	eccentric, pointing windward
Soft rime	200-600	white	eccentric pointing windward

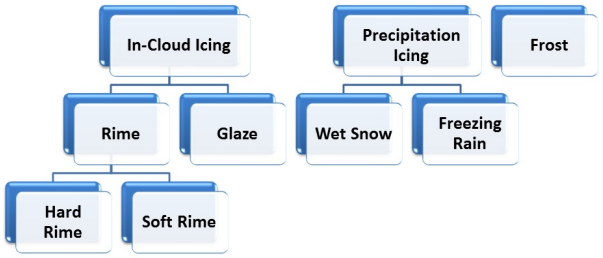

(a) Ice types

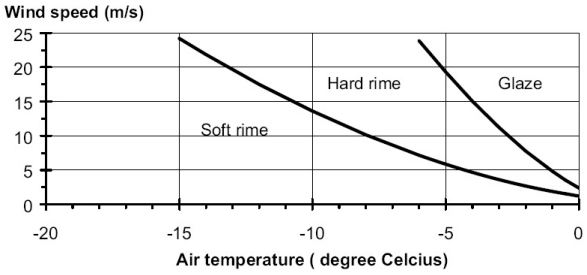

(b) Ice as a function of wind speed and air temperature

Figure 1: Ice types and their dependence [6]

(a) Precipitation icing (including freezing precipation and wet snow),
(b) In-cloud icing (also called rime/glaze, including fog),

Fig. 1(b) shows the type of accreted ice as a function of wind speed and temperature. In this figure, the curve shifts to the left with the increasing liquid water content and with decreasing object size. A classification of atmospheric ice is shown in Table I.

B. Atmospheric icing sensors

A robust technique to detect icing and ice accretion rates has not yet been reported in the published literature. It is a challenging task to devise a measurement technique that

 ISBN: 978-1-61208-207-3

can deal with both rime and glaze icing and can measure icing rate, load and duration without being affected by the icing event. Currently, all the ice detectors available are capable of measuring either one or both phenomenon such as detecting the icing event and measuring the rate of icing. As ice sensors can be integrated with ice mitigation systems, it is important for these sensors to deliver the necessary information timely enough so as to be able to operate anti-icing and de-icing mitigation strategies effectively. To distinguish between snow and ice can be considered to be an important factor for the determination of deicing power requirements. Hence, measurement of an icing event or related phenomena bounds a set of requirements which include the ability of a sensor/probe to detect icing with high sensitivity without being influenced by the icing incident. Icing measurement techniques can be classified into direct and indirect methods as follows:

Indirect Methods: The indirect methods of ice detection involve measuring weather conditions such as humidity, and temperature that lead to icing or detecting the effects of icing, for example, reduction in the power generated by the wind turbine, reduction in the speed of anemometers or measuring the variables that cause icing or variables that correlate with the occurrence of icing, such as cloud height and visibility [5] . Empirical or deterministic models are then used to determine when icing is occurring. Also Homola et. al. [7] have outlined five indirect measurement methods. The reduction in the speeds of anemometers method of Craig and Craig [2] and the noise generation frequency method of Seifert [14] are typical examples of indirect methods.

Direct Methods: The direct methods of ice and snow detection are based on the principle of detecting property changes caused by accretion such as mass, dielectric constants, conductivities, or inductance. Although Homola et. al. [7] outlined twenty four direct measurement methods but they still need to be more categorized for further exploration. The categorization of these direct methods can be,

1) Capacitive techniques
2) Microwave techniques
3) Inductance techiques
4) Ultrasonic techniques
5) Acoustic techniqes
6) Infrared techniques
7) Resonance techniques

II. Capacitive sensing technique - In general

From the above categories, the capacitive technique is the main focus of this review. The capacitance depends on the geometrical arrangement of the conductors and on the dielectric material between them, $C = C(\epsilon, G)$. For example, for a capacitor formed by n equal parallel plane plates having a geometry G depending upon area A, with a distance d between each pair, and an interposed material with a relative dielectric constant ϵ_r, the capacitance is

$$C = \epsilon_\circ \epsilon_r \frac{A}{d}(n-1)$$

where $\epsilon_\circ = 8.85pF/m$ is the dielectric constant for vacuum mentioned by Pallace and Webster [13]. Therefore, any measurand producing a variation in ϵ_r, A, or d will result in the change in the capacitance C and can be in principle sensed by that device.

A. Dielectric constant from electronic polarization

The electron orbiting a nucleus is like a harmonic oscillation with a natural frequency ω_o mentioned in Kao [9]. The dynamic equation can be defined as,

$$m\frac{d^2\Delta x}{dt^2} = -\gamma\Delta x - ZqF_{loc} \tag{1}$$

where Δx is the electrons displacement, m is the electron mass, q is the electronic charge, Z is the number electrons involved, F_{loc} is the local field acting on the atoms, and γ is the force constant. Also the natural oscillation frequency is given as $\omega_o = \sqrt{\frac{\gamma}{m}}$. Also oscillating electron is equivalent to an electric dipole and would radiate energy according to electromagnetic theory of radiation. This energy can be taken as a damping mechanism and $\beta\frac{dx}{dt}$ is a retarding force, hence our dynamic equation is,

$$m\frac{d^2\Delta x}{dt^2} + m\omega_o^2\Delta x = -\beta\frac{dx}{dt} - ZqF_{loc} \tag{2}$$

From Bohr's Model, we have the potential of electron given as,

$$E = \hbar\omega_o = \frac{mq^4}{(4\pi\varepsilon_o)^2\hbar^2} \tag{3}$$

where $\hbar = \frac{h}{2\pi}$ and h is plank's constant. Also when $Z = 1$ we have electronic polarization, $\alpha_e = 4\pi\varepsilon_o R^3$ where R is radius of the ground state orbit of Bohr's atom.
Similarly, electronic susceptibility and dielectric constant is given as,

$$\begin{aligned} \chi_e &= \frac{N\alpha_e}{\varepsilon_o} = \frac{N}{\varepsilon_o}\left[\frac{(Zq)^2}{m\omega_o^2}\right] \\ \varepsilon_r &= 1 + \chi_e = 1 + \frac{N}{\varepsilon_o}\left[\frac{(Zq)^2}{m\omega_o^2}\right] \end{aligned} \tag{4}$$

B. Complex dielectric constant

When a time varying electric field is applied across a parallel plate capacitor with the plate area of one unit and a separation of d between the plates, then the total current is given by,

$$J_T = J + \frac{dD}{dt} = J + \varepsilon^*\frac{dF}{dt} \tag{5}$$

where J is the conduction current and ε^* is defined as complex permittivity which is introduced to allow for dielectric losses due to friction accompanying polarization and orientation of electric dipoles. This may be written as,

$$\varepsilon^* = \varepsilon - j\varepsilon' = \left(\varepsilon_r - j\varepsilon_r'\right)\varepsilon_o \tag{6}$$

 ISBN: 978-1-61208-207-3

where ε_r is dielectric constant and $\varepsilon_r^{'}$ is the loss factor. Also loss tangent is defined as, $\tan\delta = \frac{\varepsilon_r^{'}}{\varepsilon_r}$ where δ is loss angle. We can use the instantaneous energy absorbed per second per cm^3 is given by $J_T(t)F(t)$. Thus, on average, the amount of energy per cm^3 per second absorbed by the material is

$$W = \frac{\omega \varepsilon_r^{'} \varepsilon_o F_m^2}{2} \tag{7}$$

The discrete nature of matter, and the behavior and interaction of those particles, can be manifested through their response to time varying electric fields with wavelengths comparable the distances between the particles. To measure the dynamic response, we can use either use,

Time Domain Approach: We measure the time dependent polarization immmediately after the application of a step function electric field or we meausre the decay of the polarization from an initial steady state value to zero after the sudden removal of an initial polarizing field. This decay is generally referred to as *dielectric relaxation*.

Frequency Domain Approach: We mainly measure the dielectric constant at various frequencies of alternating excitation fields. From the viewpoint of measuring techniques, the time domain approach is simpler than the frequency domain approach, but from the viewpoint of data analysis, the time domain approach is more complex. However, both approaches should be intimately connected and should yield, in principle, the same results.

1) Dielectric relaxation - Time Domain Approach: This is a time domain approach which provides conspicuous information abouth the nonlinearity of the dielectric behavior simply by varying the amplitude of the applied step function held. Experimental arrangement for the measurements of the time domain response (i.e., the transient charging or discharging current, resulting from the application or the removal of a step DC voltage) is given in Fig. 2.

In this circuit, the switch S_1 has 2 positions: one for turning on the step DC voltage to start the flow of charging current, the other for short circuiting the specimen to allow the discharging current to flow after the specimen has been fully charged to a steady state level. The switch S_2 is used to short circuit R_1 to provide a path for surge currents for a very short period of time to protect the circuit; it also gives a chance to adjust the amplifier to a null position before recording the transient current. It is important to make the time constant of the amplifier which depends on the stray capacitance in shunt with R_1, much smaller than the time during which the transient current is flowing. The specimen has the guard and the guarded electrodes, the outer guard electrode being connected to ground to eliminate surface leakage currents from the specimen. The charging or discharging current is measured as a voltage appearing across R_1 by means of a DC amplifier. The voltage drop from point A to ground is made zero by a negative feedback in the amplifier circuit, which produces a voltage across R_2 equal and opposite to that across R_1 thus making the applied step voltage across the specimen only. The step voltage and the charging and discharging current as a function of time are also shown in Fig. 2(b) in which $I_\circ$ is the steady DC compoent of the charging current and the width of the step voltage is 63 seconds.

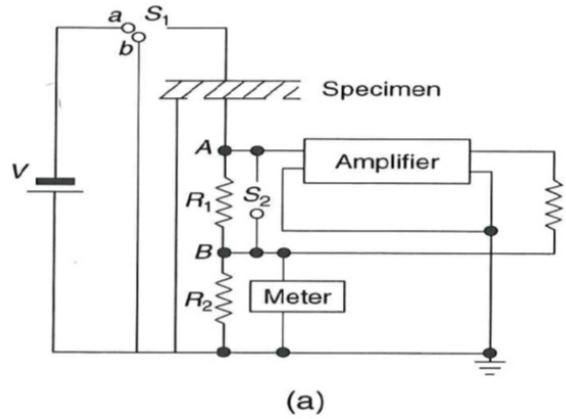

(a)

(a) Basic experimental arrangement

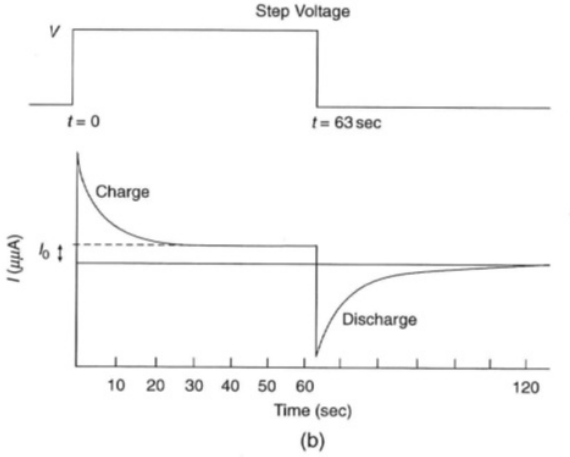

(b)

(b) The step voltage and responses

Figure 2: Setup for the measurements of the charging and the discharging current from the application and removal of a step voltage [9]

2) Frequency Domain Approach: No material is free of dielectric losses and therefore no material is free of absorption and dispersion which reflects that no material is frequency independent ε_r and $\varepsilon_r^{'}$. Now, using Debye Equations for a varying electric field $F_m e^{j\omega t}$ we have the relationships as,

$$\varepsilon_r = \varepsilon_{r\infty} + \frac{\varepsilon_{rs} + \varepsilon_{r\infty}}{1 + \omega^2 \tau_0^2} \tag{8}$$

$$\varepsilon_r^{'} = \frac{(\varepsilon_{rs} - \varepsilon_{r\infty})\,\omega\tau_0}{1 + \omega^2 \tau_0^2} \tag{9}$$

$$\tan\delta = \frac{\varepsilon_r^{'}}{\varepsilon_r} = \frac{(\varepsilon_{rs} - \varepsilon_{r\infty})\,\omega\tau_0}{\varepsilon_{rs} + \varepsilon_{r\infty}\omega^2\tau_0^2} \tag{10}$$

Eq(s). 8, 9, 10 equations can also be written as,

$$\frac{\varepsilon_r - \varepsilon_{r\infty}}{\varepsilon_{rs} - \varepsilon_{r\infty}} = \frac{1}{1+\omega^2\tau_0^2} \tag{11}$$

$$\frac{\varepsilon_r^{'}}{\varepsilon_{rs} - \varepsilon_{r\infty}} = \frac{\omega\tau_0}{1+\omega^2\tau_0^2} \tag{12}$$

Now, the Eqn(s). 11, 12 are the parametric equations of a circle in the $\varepsilon_r - \varepsilon_r^{'}$ plane. By eliminating $\omega\tau_0$ from Eq. 11 and 12 we obtain,

$$\left(\varepsilon_r - \frac{\varepsilon_{rs}+\varepsilon_{r\infty}}{2}\right)^2 + \varepsilon_r^{'2} = \left(\frac{\varepsilon_{rs}-\varepsilon_{r\infty}}{2}\right)^2 \tag{13}$$

Only the semicircle of Eqn(s). 13 over which $\varepsilon_r^{'}$ is positive has physical significance. In this Argand Diagram shown in Fig. 3(b), frequency is not explicitly shown. The variation of ε_r and $\varepsilon_r^{'}$ due to the variation of ω is shown in Fig. 3(a) which illustrates schematically the typical dispersion behavior for polarization in the relaxation regime. Also, the Eq(s). 8, 9, 10 are based on the following assumptions for simplicity: the local field is the same as the applied field F; the conductivity of the materials is negligible; all dipoles have only one identical relaxation time $\tau_\circ$. For more details on the mathematical description of the various forms of Debye relations for the detection of atmospheric ice, see Mughal et. al. [11].

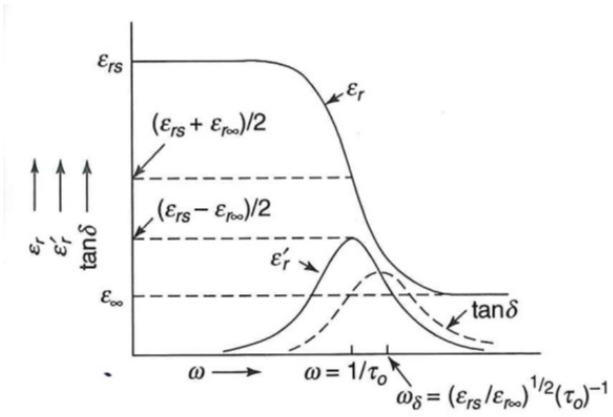

(a) ε_r , $\varepsilon_r^{'}$ and $tan\delta$ as functions of ω

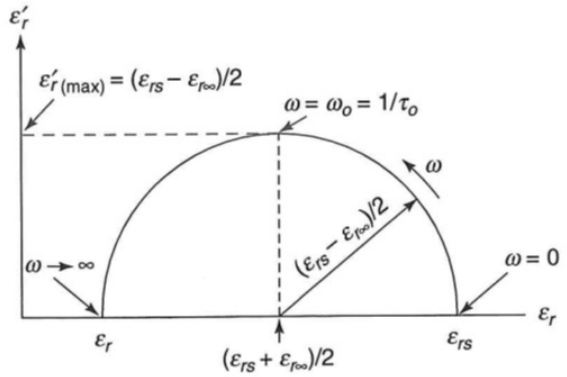

(b) Argand diagram of $\varepsilon_r - \varepsilon_r^{'}$ relations for cases with one one relaxation time $\tau_\circ$

Figure 3: Frequency domain approach for measurement of dielectric constants [9]

III. Capacitive icing sensors

Capacitive ice sensors generate an electric field to detect the presence of dielectric materials. Such electric field radiates outward around the probe and a dielectric material in close proximity of the field affects the measured capacitance, Mughal et. al. [10]. This attribute enables non-invasive measurements. In Tiuri et. al. [15], the results indicate that the complex dielectric constant is practically independent of the structure of snow. It is also mentioned that for dry snow, the dielectric constant is determined by the density and for wet snow, the imaginary part and the increase of the real part due to liquid water have the same volumetric wetness dependence. The static dielectric constants, ε_0 of both polycrystalline and single crystals of ice have been carefully determined Auty and Cole [1]. Also, application electrical properties to the measurement of ice thickness, temperature, crystal orientations are presented in Evanes [4]. Weinstein [16], Kwadwo [12] and Jarvinen [8] proposed three different capacitive based ice detection methods, Mughal et. al. [10], which are discussed in the following sections.

A. Capacitive ice detector by Weinstein

This ice sensor proposed by Weinstein [16] as given in Fig(s). 4a(a) can be used for the determination of the thickness of ice (22) on the outer surface (12) of an object independent of temperature and the composition of the ice (22). First capacitive guage (16), second capacitive guage (18), and the temperature guage (20) are embedded in embedding material (14) located within a hollow portion of outer surface (12). First capacitive guage (16), second capacitive guage (18), and temperature guage (20) are respectively connected to first capacitance measurement circuit (24), second capacitance measurement circuit (26), and temperature measuring circuit (28). The geometry of first and second capacitive guages (16) and (18) is such that the ratio of voltage outputs of first and second capacitive guages (24) and (26) is proportional to the thickness of ice (22), regardless of ice temperature or composition. This ratio is determined by offset and dividing circuit (29). First capacitance measuring circuit (24) and second capacitance measuring circuit (26) are connected to offset the dividing circuit (29). The output voltage V_{out} of this offset and dividing circuit (29) for ice conditions is determined by the relation,

$$V_{out} = \frac{(V - V_o)_2}{(V - V_o)_1} \tag{14}$$

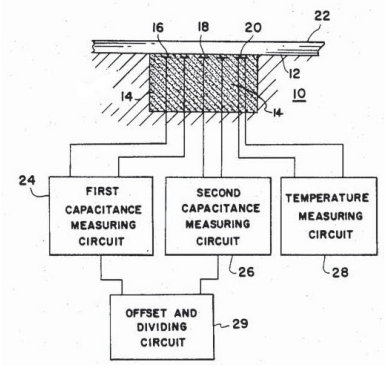

(a) Construction

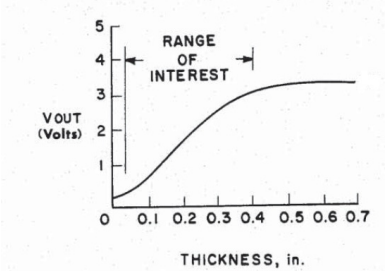

(b) Ratio of capacitance gauge as a function of thickness

Figure 4: Weinstein ice detector [16]

where V is the voltage output for the ice conditions and V_o is the initial voltage for no ice conditions. Subscripts (1) and (2) refer respectively to capactive measurements from first capacitance measuring circuit (24) and second capacitance measurement circuit (26). V_{out} is independent of both temperature and ice decomposition since both effects results in identical scaling factors for both $\frac{V-V_o}{2}$ and $V - V_{o1}$, thereby resulting no changes in Eq(s). 14. The variation of capacitance as a function of thickness is shown in Fig(s). 4a(b). *This sensor is capable of predicting ice and its thickness on a planar surface*.

B. Two cylinder capacitive icing probe

Kwadwo [12] has used two-cylinder probes to act as a capacitive ice sensor, based on the principle that as ice accretes on two electrically charged parallel-arranged cylindrical probes, the measured capacitance increases, while the resistance decreases. As the super cooled water droplets collide with the cylindrical probes and stick on the surface, they freeze and ice begins to grow as shown in Fig 5b. The accreted ice affects the electric field generated by the electrically charged cylindrical probes resulting in an increase in the capacitance due to the higher dielectric constant of the accreted ice compared to air. The electric field originating from the polarization charges on the surface of the ice partly shields the external electric field generated by the charged cylindrical probes leading to a reduction in the overall electric field. The overall voltage decreases simultaneously, because the electric field is directly proportional to the voltage. The resistance between the cylindrical probes is large at the start of the icing event because of the air gap between the cylinders. However, as ice builds up on the cylindrical probes, the air gap between the cylindrical probes decreases and the resistance begins to decrease exponentially. The rate of decrease is sensitive to the presence of water on the surface of the ice formed on the cylindrical probes and this phenomenon is used to distinguish between different types of ice .

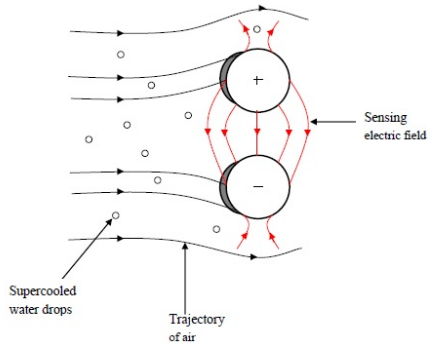

(a) Trajectory of supercooled water drops and air moving towards two cylindrical probes

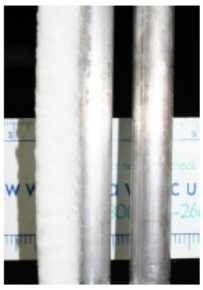

(b) Ice formation at the windward side of the cylindrical probes

Figure 5: Cylindrical capacitive sensor

C. Total impedance and complex dielectric property ice detection system

In this sensor, Jarvinen [8] used the method for detecting the presence and the accretion of ice by first measuring the properties of the contaminant layer overlying the ice sensor. The contaminant layer's temperature, thermal conductivity and variation of total impedance versus ice sensor electrical excitation frequency are measured. The complex dielectric property subsystem monitors the dielectric property locus in dielectric space as the excitation frequency is varied from near dc to higher frequencies (using Cole-Cole plot) and compares the measured results for magnitude and shape with laboratory property data taken at the same temperature and stored in the processor. It double checks using external ice (based upon the complex dielectric measurements) sensor

 ISBN: 978-1-61208-207-3

whether it is ice or rain water or deicing fluid or snow. If the measured results form a semicircular shaped locus of dielectric properties in complex dielectric space during the frequency scan and those measurements are also determined to be in agreement with on board stored laboratory ice data, ice is confirmed to be present. The presence of ice is also confirmed if a particular vector can be constructed from the measured data taken at a single preselected excitation frequency and found to have a vector angle in agreement with the vector angle from stored laboratory results taken at the same measurement conditions. In addition, complex dielectric measurement algorithms identify whether cracks, flaws or voids or increased electrical conductivity exist in the ice covering and sensor from their effects on the shape and size of the measured complex dielectric locus or from the length of the vector at the pre selected frequency. The presence of flaws, cracks or voids or enhanced electrical conductivity are determined from the values for the low frequency and high frequency intercepts and the value for diameter of the complex dielectric locus if these values are found to differ from those calculated for ice based on stored ice data. These differences, if found to exist, are used to correct the initially chosen ice thickness value based on the assumption of normal ice: ice with no flaws, cracks or voids or higher electrical conductivity. For more details on the mathematical principle of this type of sensing technique see Mugal et. al. [11].

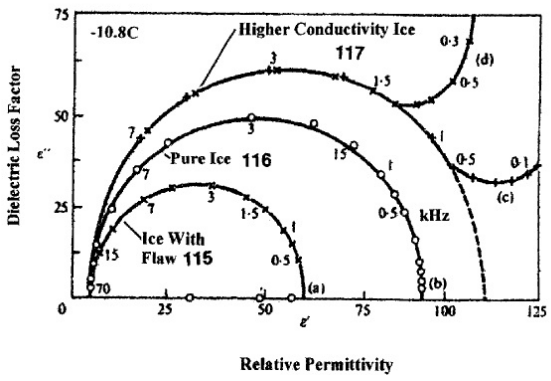

Figure 6: Cole Cole plot for glaze ice experimental results

This sensor is capable to identify the presence of ice, its thickness, thickness rate, and can identify glaze ice, rime ice, rain water, deicing fluid, snow or air. In addition it is redundant in confirming the icing event.

IV. Conclusion and Future Work

The mere existence of a permanent dipole moment in water provides structural information about the molecule. It is found that the dielectric variations in different types of ice can be very effective in finding the parameters such as ice type, ice thickness and icing rate. The patent of Jaravinen [8] can be considered as a benchmark as it is able to sense all the above paramters, hence the direct approach mentioned by Homola et. al. [7] is able to deliver maximum information. Also due to the variation in response of ice and snow by varying the electrical field; the application of Cole-Cole Diagram for complex dielectric constant of snow and ice is adequately proved. It is stressed that a simulation study and analytical study on the capacitive variations of atmospheric ice be carried out to compare the numerical and theoretical results with the experimental variations. These results can further be utilized for the determination of atmospheric ice type and measurement of its rate and thickness. A hybrid measurement technique may also be considered in future for robust results.

Acknowledgements

The work reported in this paper was partially funded by the Research Council of Norway, project no. 195153/160 and partially by the consortium of the ColdTech project - Sustainable Cold Climate Technology.

References

[1] Auty R. P. and Cole R. H., "Dielectric properties of ice and solid D_2O", Journal of Chemical Physics, Vol. 20, Issue 8, pp. 1309-1314, 1952.

[2] Craig D. F. and Craig D. B., "An investigation of icing events on haeckel hill", Proceedings of Boreas III Conference, Finland, 1995.

[3] Eisenberg D. and Kauzmann W. "The Structure and Properties of Water", Oxford University Press, 1969.

[4] Evanes S., "Dielectric properties of ice and snow - a review", Journal of glaciology, Vol. 5, Issue 42, pp. 773-792, 1965.

[5] Fikke S., et. al., "Cost 727 - Atmospheric icing on structures; measurement and data collection on icing", ISSN 1422-1381, MeteoSwiss, 2007.

[6] Foder H. F., "ISO 12494 - Atmospheric icing on structures and how to use it", Proc. of the 11th International Offshore and Polar Engineering Conference, ISBN 1-880653-51-6, June 2001.

[7] Homola M. C., Nicklasson P. J., and Sundsbo P.A., "Ice sensors for wind turbines", Cold Regions Science and Technology, 46: pp. 125-131, 2006.

[8] Jarvinen P. O., "Total impedience and complex dielectric property ice detection system", US Patent 7439877, 2008.

[9] Kao K. C., "Dielectric phenomena in solids", Elsevier Academic Press, ISBN 0-12-396561-6, 2004.

[10] Mughal U. N., Virk M. S., and Mustafa M. Y., "Review Of Atmospheric Ice Detection Techniques", unpublished.

[11] Mughal U. N., Virk M. S., and Mustafa M. Y., "Dielectric Based Sensing Of Atmospheric Ice", 38th International Conference on Application of Mathematics in Engineering and Economics, AIP Conference Proceedings, in press.

[12] Owusu K. P., "Capacitive probe for ice detection and accretion rate measurement: proof of concept", Masters thesis report submitted at University of Mannitoba, 2010.

[13] Pallas-Areny R. and Webster J. G., "Sensors and signal conditioning", 2nd Edition, John Wiley and & Sons, 2001.

[14] Seifert H., "Technical Requirements for Rotor Blades Operating in Cold Climates", Proceedings of the BOREAS II conference, Pyhatunturi, Finland, 2003.

[15] Tiuri M., Sihvola A., Nyfors E., and Hallikaiken M., "The complex dielectric constant of snow at microwave frequencies", IEEE Journal of Oceanic Engineering, Vol. 9, Issue 5, pp. 377 - 382, 1984.

[16] Weinstein L. M., "Ice sensor", US Patent 4766369, 1988.

 ISBN: 978-1-61208-207-3